Skeletal Radiology (2019) 48:1815–1820
https://doi.org/10.1007/s00256-019-03199-9

CASE REPORT

Epithelioid schwannoma: imaging findings on radiographs, MRI, and ultrasound

Hillary W. Garner[1] · Benjamin K. Wilke[2] · Karen Fritchie[3] · Joseph M. Bestic[1]

Received: 28 December 2018 / Revised: 21 February 2019 / Accepted: 26 February 2019 / Published online: 22 March 2019

Abstract

Epithelioid schwannoma is an uncommon benign peripheral nerve sheath tumor, with distinct morphological and pathological features. To our knowledge, the imaging features of epithelioid schwannoma have not been described. In this case report, we describe the imaging findings of a pathologically proven case of epithelioid schwannoma presenting as a slowly growing painless mass near the ankle. The MR imaging signs commonly associated with conventional schwannoma were absent. On correlative radiographs, there were intra-tumoral calcifications. Radiographs are an essential tool in the imaging evaluation of soft-tissue masses. Knowledge of soft-tissue tumor types that can be associated with intra-tumoral calcifications is helpful in honing the differential diagnosis.

Keywords Schwannoma · Epithelioid · Radiographs · MRI · Ultrasound · Soft tissue · Neoplasm

Introduction

Schwannoma is a common benign peripheral nerve sheath tumor, representing approximately 5% of all benign soft-tissue tumors [1, 2]. These mesenchymal tumors arise from Schwann cells and in their conventional form demonstrate characteristic imaging and pathological features. However, there are several rare morphological variants of schwannoma that can confound the diagnosis. These include epithelioid, cellular, plexiform, microcystic/reticular, and neuroblastoma-like schwannoma [3]. Such variants demonstrate histological features that may suggest a more aggressive biological behavior. Therefore, recognition of these variants is important for appropriate treatment stratification and follow-up. Immunohistochemical analytic capabilities have progressed in recent years, allowing for more accurate differentiation of these subtypes and their more aggressive counterparts. Although over 140 cases of epithelioid schwannoma (ES) have been reported in the pathology literature [4–13], the imaging characteristics of this variant have not been described.

We report a case of ES in the soft tissues of the ankle that was diagnosed utilizing morphological and immunohistochemical analyses. The imaging findings were indeterminate in isolation, but were concordant with the pathological diagnosis upon multidisciplinary review. We highlight the reasoning behind the imaging differential diagnosis, particularly emphasizing the presence of intra-tumoral calcification and the essential value that radiographs provide for any patient presenting with a soft-tissue mass.

Case report

The patient is a healthy 38-year-old man who presented to an outside podiatrist with a slowly growing painless mass in the right ankle region, which he first noticed 6 months before presentation. Magnetic resonance imaging (MRI) of the right ankle was performed at an outside institution and revealed a soft-tissue mass. The patient was subsequently referred to our orthopedic oncologist, who requested right ankle radiographs. The lateral radiograph (Fig. 1) demonstrated soft-tissue fullness overlying the expected locations of the distal flexor myotendinous junctions and tarsal tunnel with several associated small, rounded, irregular calcifications. The outside MRI (Fig. 2) of the right ankle demonstrated an oblong well-

✉ Hillary W. Garner
garner.hillary@mayo.edu

[1] Department of Radiology, Mayo Clinic, 4500 San Pablo Road, Jacksonville, FL 32224, USA

[2] Department of Orthopedic Surgery, Mayo Clinic, 4500 San Pablo Road, Jacksonville, FL 32224, USA

[3] Department of Laboratory Medicine and Pathology, Mayo Clinic, 200 1st Street SW, Rochester, MN 55905, USA

Fig. 1 Lateral radiograph of the right ankle demonstrates soft-tissue fullness (*arrows*) overlying the expected locations of the distal flexor myotendinous junctions and tarsal tunnel with several associated small, irregular, rounded, irregular calcifications

circumscribed soft-tissue mass centered between the flexor hallucis longus myotendinous junction and the tarsal tunnel. The mass was in close proximity to the posterior tibial nerve, but at their closest approximation, there was a very thin fat plane between the mass and nerve on the axial T1-weighted images. The mass was isointense to slightly hyperintense to muscle on a T1-weighted image (Fig. 2a), heterogeneous but primarily hyperintense on a T2-weighted image (Fig. 2b), and demonstrated heterogeneous enhancement (Fig. 2c). Given its shape and proximity to the posterior tibial nerve, a benign peripheral nerve sheath tumor was a diagnostic consideration. However, it lacked some of the characteristic imaging features of benign nerve sheath tumors, such as the "target" sign (T2 hyperintense rim surrounding a central area of low signal) and the "split fat" sign (tapered rim of fat signal adjacent to the proximal and distal ends of the mass). Ancient schwannoma was a consideration because of the calcification, but it lacked the extensive signal heterogeneity often associated with this diagnosis. Synovial sarcoma was therefore favored in the differential diagnosis owing to the presence of intra-tumoral calcification and its periarticular location. Other rarer calcifying soft-tissue sarcomas, such as mesenchymal chondrosarcoma, were considered unlikely. Owing to the indeterminate imaging features of the mass, a biopsy was indicated.

An ultrasound-guided biopsy of the mass was performed. Preliminary ultrasound images (Fig. 3) showed a predominantly hypoechoic, well-circumscribed mass with no internal vascularity. The mass contained several small hyperechoic areas with associated posterior acoustic shadowing, which corresponded to the calcifications seen

Fig. 2 **a** Sagittal T1-weighted image of the right ankle demonstrates an oblong well-circumscribed soft-tissue mass (*arrows*) that was isointense to slightly hyperintense to muscle. **b** Axial T2-weighted fat-saturated image and **c** axial T1-weighted fat-saturated post-contrast image of the right ankle show the mass (*arrows*) was centered between the flexor hallucis longus myotendinous junction and the tarsal tunnel. The mass demonstrated heterogeneous but primarily hyperintense T2 signal, with the T2 hyperintense areas likely reflective of the myxoid matrix and the T2 hypointense areas likely reflective of the hyalinized matrix seen histopathologically. The mass was also heterogeneously enhancing. The mass was in close proximity to the posterior tibial nerve (*arrowheads* in **a**–**c**), but at their closest approximation, there was a very thin fat plane between the mass and nerve on the axial T1 images (not shown)

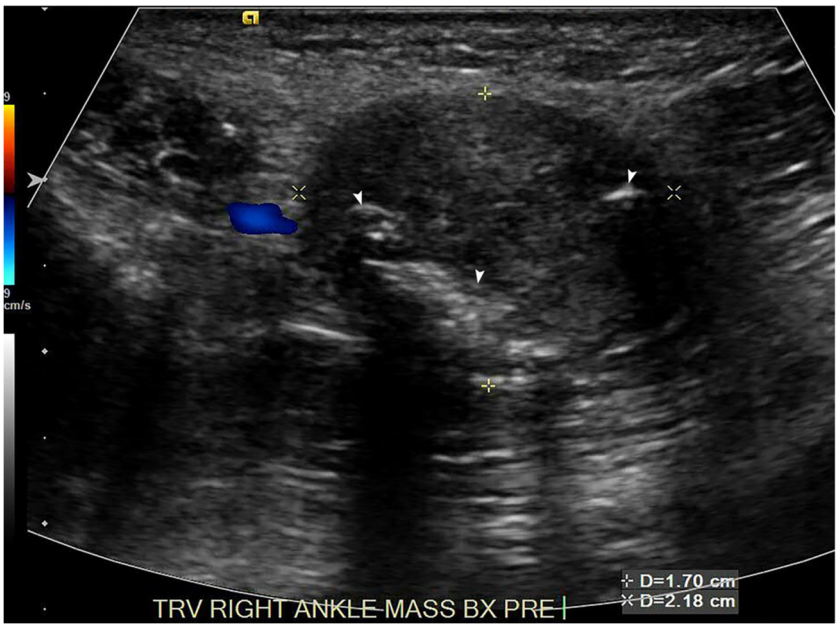

Fig. 3 Ultrasound Doppler image of the right posterior ankle region demonstrates a predominantly hypoechoic, well-circumscribed mass with no internal vascularity. The mass contained several small hyperechoic areas (*arrowheads*) with associated posterior acoustic shadowing, which corresponded to the calcifications seen radiographically

radiographically. Three core biopsy samples were obtained using a 14-gauge device.

The histopathology from the biopsy specimen revealed a proliferation of nests and strands of plump epithelioid cells with hyperchromatic nuclei and intranuclear inclusions (Fig. 4a). The tumor cells were deposited in a predominantly hyalinized matrix admixed with thick-walled blood vessels (Fig. 4b). Although mild degenerative atypia was noted, severe cytological atypia was absent, and mitotic figures were difficult to find. No necrosis was appreciated. The immunoprofile of the tumor cells demonstrated strong and diffuse S100 positivity and loss of SMARCB/INI-1 expression (Fig. 4c, d). The tumor cells were negative for cytokeratin, OSCAR, desmin, melan-A, and HMB45. The morphological and histological features were compatible with an ES. The patient was evaluated for other lesions to exclude the possibility of schwannomatosis, but this mass was the only lesion.

Following discussion with the orthopedic oncologist, the patient elected to undergo a marginal surgical excision as the mass was symptomatic when wearing shoes. The mass was approached through a posteromedial incision with identification and protection of the tibial nerve and posterior tibial artery and vein (Fig. 5a). The proximal and distal ends of the small nerve from which the ES emanated were identified (Fig. 5b, c). The ES was then excised without difficulty (Fig. 5d).

The final histopathology revealed a well-circumscribed and encapsulated multilobulated lesion composed of epithelioid cells with similar features to those appreciated on the previous biopsy (Fig. 6a). Numerous foci of dystrophic calcification were also noted (Fig. 6b). The surgical margins were negative.

The patient recovered quickly from surgery and has had no postoperative complications in the 5 months since resection. Owing to the low risk of recurrence, no follow-up has been preemptively scheduled.

Discussion

Epithelioid schwannomas most often present as a solitary subcutaneous mass involving the extremities in middle adulthood [13]. These tumors are almost always benign, but there have been occasional reports of transformation to epithelioid malignant peripheral nerve sheath tumors [7, 9, 12–14]. Although the lesional cells of conventional schwannoma are typically spindled, this variant harbors predominantly plump epithelioid Schwann cells organized in clusters, nests, and cords within the variably hyalinized and myxoid background. The features of ordinary schwannoma, such as encapsulation, nuclear palisading, and ectatic blood vessels, are often present. The mitotic rate is usually ≤2 mitotic figures/10 high power field, and necrosis is absent. The epithelioid Schwann cell population exhibits strong and diffuse S100/SOX10 staining by immunohistochemistry. Recent work by Jo and Fletcher has shown that approximately 40% of ESs show loss of SMARCB1/INI1 expression. In contrast, 95% of sporadic conventional schwannomas show retention of SMARCB1/INI1 expression [13]. Of note, ES is almost always sporadic, with only one case of ES associated with schwannomatosis reported in the two largest series of ES [12, 13].

Treatment of ESs includes observation for asymptomatic lesions. If the lesion is causing symptoms then surgical excision may be indicated. A marginal excision is often performed due to the benign nature of the lesion. Careful dissection is required to dissect the schwannoma free from the underlying

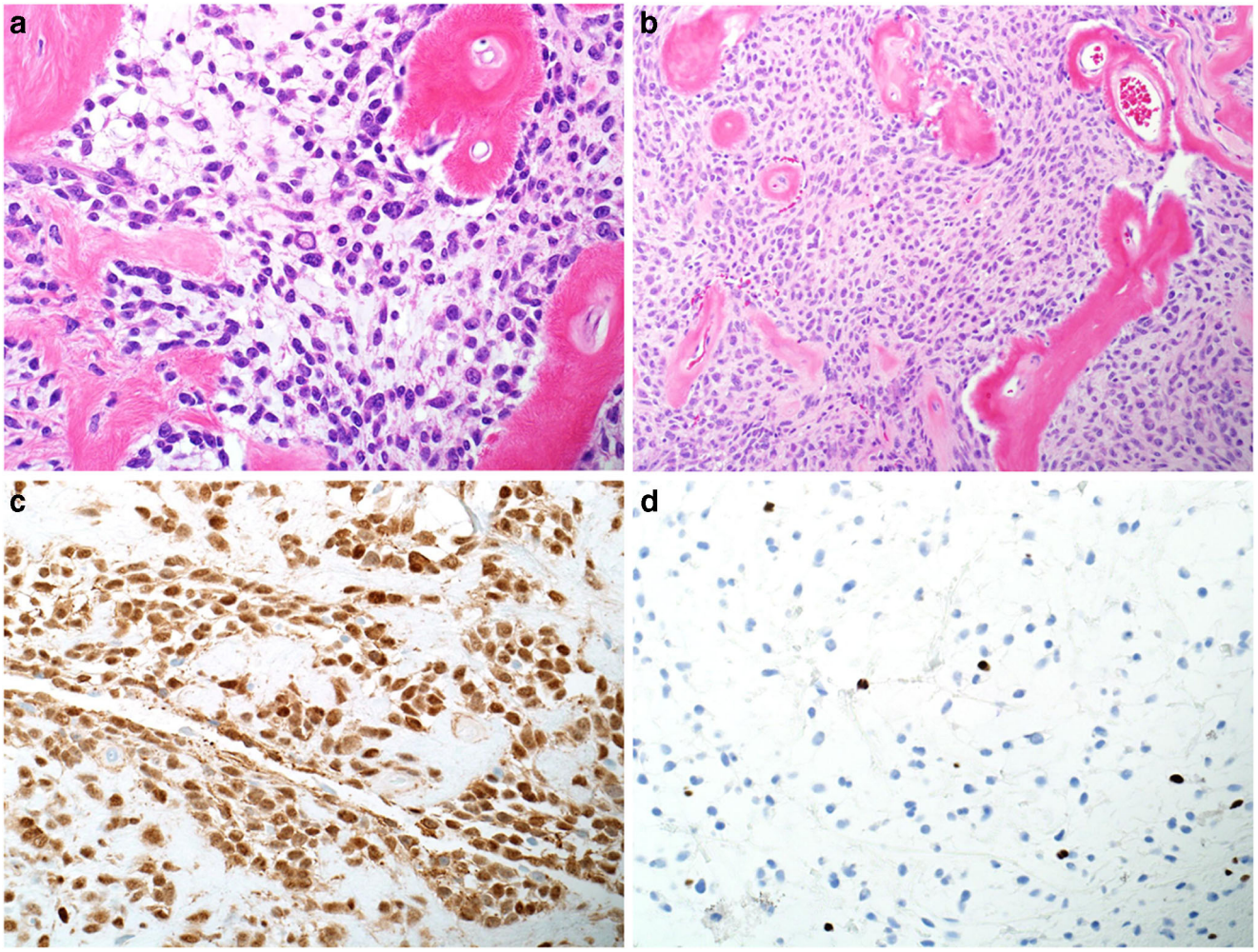

Fig. 4 **a** Histopathology of the biopsy specimen (hematoxylin and eosin; ×40 magnification) demonstrates a proliferation of nests and strands of plump epithelioid cells with hyperchromatic nuclei and intranuclear inclusions. **b** Histopathology of the biopsy specimen (hematoxylin and eosin; ×20 magnification) shows the tumor cells were deposited in a predominantly hyalinized matrix admixed with thick-walled blood vessels. Most of the cells visualized in **a** and **b** are epithelioid. **c** Immunoprofile with S100 of the biopsy specimen (×40 magnification) demonstrates strong and diffuse S100 positivity of the tumor cells. **d** Immunoprofile with INI-1 of the biopsy specimen (×40 magnification) shows loss of SMARCB/INI-1 expression

nerve fascicles to prevent sensory or motor deficits. Recurrence following excision is rare [12].

Although ES has been addressed in the histopathology and surgery literature, imaging findings of this schwannoma variant have not been described. Three case reports [15–17] of ES, 2 intracranial and 1 spinal, do include figures with selected MRI. However, the imaging characteristics of the masses are not fully illustrated or described, precluding accurate comparison with the case presented here. In our case, the mildly heterogeneous nature of the mass on T2-weighted imaging, with areas of both hyperintensity and hypointensity, are likely reflective of the admixture of myxoid matrix and hyalinized matrix respectively (Fig. 6a).

In general, accurate diagnosis of soft-tissue tumors can be significantly enhanced with multidisciplinary radiology–histopathology correlation. This is particularly true with regard to rare atypical tumors, where both radiologists and pathologists may be relatively unfamiliar with the tumor characteristics. Although the imaging features of most soft-tissue tumors are nonspecific, the presence of calcification within a soft-tissue mass is unusual enough that it can help to hone the differential diagnosis.

In a study of 454 patients who had soft-tissue masses and corresponding radiographs, Gartner et al. [18] reported that 76 (16.7%) patients had associated intra-tumoral calcification, which they classified as ossification, chondroid calcification, phleboliths, and "other." There were two cases in their study group of schwannoma with intra-tumoral calcification, the first containing calcifications classified as phleboliths and the second containing calcifications classified as "other." In general, calcification within schwannomas is considered a product of degeneration and is therefore most often

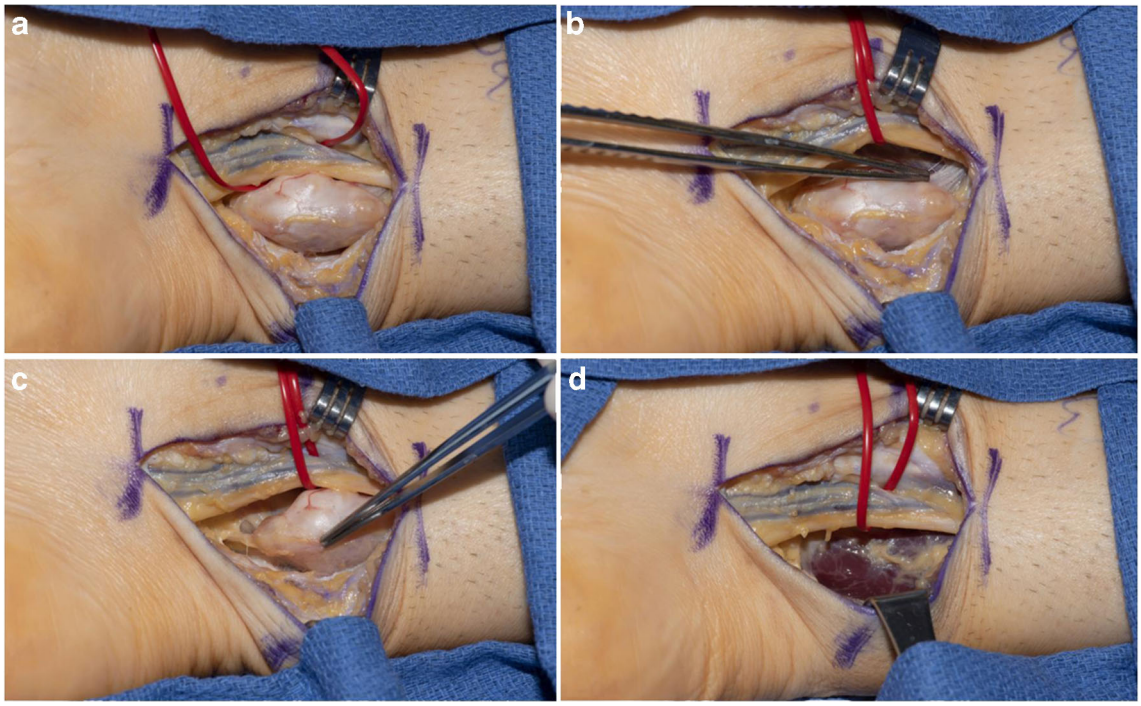

Fig. 5 **a** A posteromedial approach to the ankle was used to expose the epithelioid schwannoma adjacent to the tibial nerve and posterior tibial vessels. **b**, **c** The proximal and distal extent of the schwannoma was identified along with the nerve branch involved. **d** The wound is shown following excision of the epithelioid schwannoma

encountered in the "ancient" variant of schwannoma. This degenerative change with hemorrhage and cyst formation can also cause extensive T1 and T2 signal heterogeneity in ancient schwannoma [19, 20]. Conversely, there are no data in the literature on the rate of calcification in ES. In the largest pathology series of ES to date [12, 13], calcifications were not described in the studied lesions.

In this particular case, the presence of intra-tumoral calcification helped to limit our differential diagnosis to synovial sarcoma and benign peripheral nerve sheath tumor, including conventional schwannoma and ancient schwannoma. Although a benign nerve sheath tumor was a consideration, the imaging features often associated with conventional schwannoma, namely the "target sign" and the "split-fat sign," were absent. The extensive

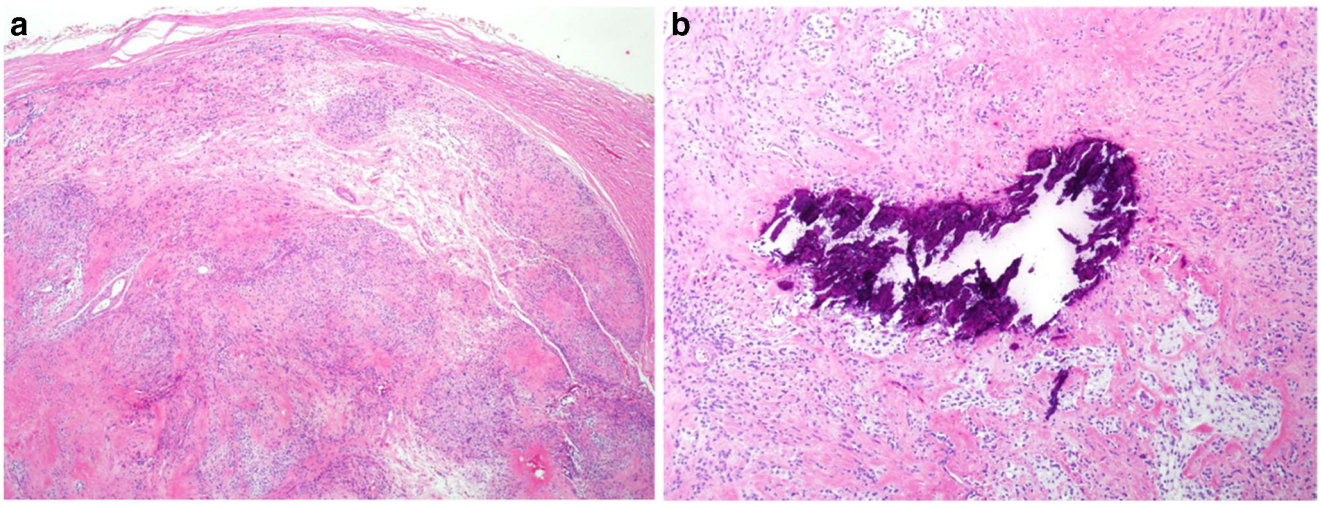

Fig. 6 **a** Histopathology of the resected mass (hematoxylin and eosin; ×4 magnification) demonstrates an encapsulated multilobulated lesion composed of epithelioid cells with similar features to those appreciated on Fig. 4a and b. **b** There is both myxoid matrix (*white areas*) and hyalinized matrix (*pink acellular areas*) within the mass. Histopathology of the resected mass (hematoxylin and eosin; ×10 magnification) shows a dystrophic calcification within the mass

signal heterogeneity we expect of ancient schwannoma was also absent. Therefore, synovial sarcoma was our working imaging diagnosis based on the periarticular location and the more common association of intra-tumoral calcification with synovial sarcoma. Despite initially favoring synovial sarcoma, the pathological diagnosis of ES was concordant given its other MRI and ultrasound imaging features. Knowledge of other soft-tissue tumors such as ES that can be associated with internal calcification, in addition to the tumors reported by Gartner et al., is valuable when atypical imaging and histopathology findings are encountered.

Soft-tissue calcifications are not readily apparent on MRI. Although diagnosis may suffer infrequently from an MRI-only approach to soft-tissue mass evaluation, there have been many situations in our practice where it has been vital to make the diagnosis and help to avoid inappropriate treatment. Therefore, we strongly advocate the use of radiographs for evaluation of all soft-tissue tumors.

In summary, this case report is unique because imaging findings of ES have not been previously described. The presence of intralesional calcification described in this case report is an important feature, in that ES can now be included in the differential diagnosis for a soft-tissue mass containing calcification. Given a relatively small number of tumors and tumor-like conditions that are known to demonstrate intra-tumoral calcifications, the presence of such calcifications effectively limits the differential considerations and can aid in establishing consensus upon multidisciplinary review.

Compliance with ethical standards

Conflicts of interest The authors declare that they have no conflicts of interest.

References

1. Kransdorf MJ. Benign soft-tissue tumors in a large referral population: distribution of specific diagnoses by age, sex, and location. Am J Roentgenol. 1995;164(2):395–402.
2. Murphey MD, Smith WS, Smith SE, Kransdorf MJ, Temple HT. From the archives of the AFIP. Imaging of musculoskeletal neurogenic tumors: radiologic-pathologic correlation. Radiographics. 1999;19:1253–80.
3. Rodriguez FJ, Folpe AL, Giannini C, Perry A. Pathology of peripheral nerve sheath tumors: diagnostic overview and update on selected diagnostic problems. Acta Neuropathol. 2012;123(3):295–319.
4. Franks AJ. Epithelioid neurilemmoma of the trigeminal nerve: an immunohistochemical and ultrastructural study. Histopathology. 1985;9(12):1339–50.
5. Orosz Z, Sapi Z, Szentirmay Z. Unusual benign neurogenic soft tissue tumour. Epithelioid schwannoma or an ossifying fibromyxoid tumour? Pathol Res Pract. 1993;189(5):601–5.
6. Cervoni L, Raguso M, De Bac S, et al. Epithelioid schwannoma of the ulnar nerve. Some clinical observations. Minerva Chir. 1998;53(4):313–6.
7. Kindblom LG, Meis-Kindblom JM, Havel G, Busch C. Benign epithelioid schwannoma. Am J Surg Pathol. 1998;22:762–70.
8. Smith K, Mezebish D, Williams JP, et al. Cutaneous epithelioid schwannomas: a rare variant of a benign peripheral nerve sheath tumor. J Cutan Pathol. 1998;25(1):50–5.
9. Laskin WB, Fetsch JF, Lasota J, et al. Benign epithelioid peripheral nerve sheath tumors of the soft tissues: clinicopathologic spectrum of 33 cases. Am J Surg Pathol. 2005;29(1):39–51.
10. Saad AG, Mutema GK, Mutasim DF. Benign cutaneous epithelioid schwannoma: case report and review of the literature. Am J Dermatopathol. 2005;27(1):45–7.
11. Rezanko T, Sari AA, Tunakan M, Calli AO, Altinboga AA. Epithelioid schwannoma of soft tissue: unusual morphological variant causing a diagnostic dilemma. Ann Diagn Pathol. 2012;16(6):521–6.
12. Hart J, Gardner JM, Edgar M, et al. Epithelioid schwannomas: an analysis of 58 cases including atypical variants. Am J Surg Pathol. 2016;40:704–13.
13. Jo VY, Fletcher CDM. SMARCB1/INI1 loss in epithelioid schwannoma: a clinicopathologic and immunohistochemical study of 65 cases. Am J Surg Pathol. 2017;41(8):1013–22.
14. Jo VY, Fletcher CDM. Epithelioid malignant peripheral nerve sheath tumor: clinicopathologic analysis of 63 cases. Am J Surg Pathol. 2015;39(5):673–82.
15. Vaubel RA, Chang HT, Fritchie K, Abell Aleff PC, Jentoft ME. Epithelioid schwannoma of a spinal nerve root. Can J Neurol Sci. 2016;43(3):430–3.
16. Tan TC, Lam PW. Epithelioid schwannoma of the vestibular nerve. Singapore Med J. 2004;45(8):393–6.
17. Yuen T, Kaye AH. Intracranial epithelioid schwannoma—a case report. J Clin Neurosci. 2004;11(1):91–5.
18. Gartner L, Pearce CJ, Saifuddin A. The role of the plain radiograph in the characterisation of soft tissue tumours. Skeletal Radiol. 2009;38(6):549–58.
19. Isobe K, Shimizu T, Akahane T, Kato H. Imaging of ancient schwannoma. AJR Am J Roentgenol. 2004;183(2):331–6.
20. Chen YH, Hsu YH, Chang HR. Intrathoracic ancient neurilemoma mimicking mesenchymal thoracic tumor. Am J Med Sci. 2013;346(5):424–6.